Connectome-based models can predict processing speed in older adults

Mengxia Gao [a,b], Clive H.Y. Wong [a,b], Huiyuan Huang [c,d], Robin Shao [a,b], Ruiwang Huang [c,d,*], Chetwyn C.H. Chan [e,*], Tatia M.C. Lee [a,b,f,g,*]

[a] The State Key Laboratory of Brain and Cognitive Sciences, The University of Hong Kong, Hong Kong, China
[b] Laboratory of Neuropsychology, The University of Hong Kong, Hong Kong, China
[c] School of Psychology, Center for the Study of Applied Psychology, Key Laboratory of Mental Health and Cognitive Science of Guangdong Province, South China Normal University, Guangzhou 510631, China
[d] Key Laboratory of Brain Cognition and Education Sciences (South China Normal University) Ministry of Education
[e] Applied Cognitive Neuroscience Laboratory, Department of Rehabilitation Sciences, The Hong Kong Polytechnic University, Hum Hom, Hong Kong
[f] Guangdong-Hong Kong-Macao Greater Bay Area Center for Brain Science and Brain-Inspired Intelligence, Guangzhou, China
[g] Laboratory of Emotion and Cognition, The Affiliated Hospital of Guangzhou Medical University, China

ARTICLE INFO

ABSTRACT

Decrement in processing speed (PS) is a primary cognitive morbidity in clinical populations and could significantly influence other cognitive functions, such as attention and memory. Verifying the usefulness of connectome-based models for predicting neurocognitive abilities has significant translational implications on clinical and aging research. In this study, we verified that resting-state functional connectivity could be used to predict PS in 99 older adults by using connectome-based predictive modeling (CPM). We identified two distinct connectome patterns across the whole brain: the fast-PS and slow-PS networks. Relative to the slow-PS network, the fast-PS network showed more within-network connectivity in the motor and visual networks and less between-network connectivity in the motor-visual, motor-subcortical/cerebellum and motor-frontoparietal networks. We further verified that the connectivity patterns for prediction of PS were also useful for predicting attention and memory in the same sample. To test the generalizability and specificity of the connectome-based predictive models, we applied these two connectome models to an independent sample of three age groups (101 younger adults, 103 middle-aged adults and 91 older adults) and confirmed these models could specifically be generalized to predict PS of the older adults, but not the younger and middle-aged adults. Taking all the findings together, the identified connectome-based predictive models are strong for predicting PS in older adults. The application of CPM to predict neurocognitive abilities can complement conventional neurocognitive assessments, bring significant clinical benefits to patient management and aid the clinical diagnoses, prognoses and management of people undergoing the aging process.

1. Introduction

Processing speed (PS), defined as how fast a person can perform a mental task (Salthouse, 2000), is one of the strongest predictors of neurocognitive status, especially in older adults (Deary et al., 2010; Salthouse and Ferrer-Caja, 2003). Its changes underpin much of the age-related decline in higher-order cognitive abilities (Finkel et al., 2009; Luo and Craik, 2008; Salthouse, 2010; Silva et al., 2018). Hence, a decrement in processing speed is a primary cognitive morbidity in clinical populations (Dow et al., 2004) and could significantly influence other cognitive functions, such as attention (Silva et al., 2018) and memory (Hedden et al., 2005; Levitt et al., 2006; Zaremba et al., 2019), in an aging population. Such deterioration in the cognitive functions has been suggested to be one of the greatest health threats of older adults

(Bishop et al., 2010), so characterizing the different levels of PS ability in older adults may aid the clinical diagnoses, prognoses and management of people undergoing the aging process. Conventionally, in clinical settings, PS is revealed in psychometric pencil-and-paper tests (e.g., Symbol Digit Modalities Test (SDMT): Smith, 1982; Digit-Symbol Substitution: McLeod et al., 1982). With the advancement of neuroimaging knowledge and methodology, brain predictive models could aid to characterize the cognitive abilities of those patients who may have difficulties in completing neuropsychological tasks. Yet, existing literature has primarily focused on exploring the correlational relationship between brain imaging features and PS (Eckert, 2011; Silva et al., 2019); studies on the feasibility of applying imaging data to build models for predicting PS in older adults have been scarce.

In constructing a neural model for PS, task-specificity and reproducibility were two major barriers for the establishment of a neural model for cognitive constructs. To overcome these barriers, a large amount of literature has successfully demonstrated that task-free fMRI could identify age-related (Hohenfeld et al., 2018; Pievani et al., 2014) and cognitive-ability neuromarkers in older adults, such as memory performance (Meskaldji et al., 2016; Sakaki et al., 2013), attention control ability (Fountain-Zaragoza et al., 2019) and cognitive scores (Buckley et al., 2017; Lin et al., 2018). Therefore, rs-fMRI is capable of generating valuable information about individual variation in neurocognitive functioning. Although some argued that the resting state is more neutral compared to the task state, rs-fMRI has been verified to serve as a baseline brain state and could be used to predict subsequent task performance (Carter et al., 2010; Sakaki et al., 2013; Siegel et al., 2016) and to predict training effects on cognitive functions after the intervention (Arnemann et al., 2015). A number of review studies have highlighted the advantages of rs-fMRI over task-fMRI: 1) rs-fMRI data are easier to collect without the requirement of specific experimental design, thus boosting data sharing across studies and sites; 2) rs-fMRI could eliminate potential confounds that are related to task performance fluctuation and variability; 3) rs-fMRI shows high test-retest reproducibility and reliability in detecting specific process in brain functions in the absence of an explicit task (e.g., default-mode network) (Fox and Greicius, 2010; Lee et al., 2013; Panchuelo et al., 2014; Van Den Heuvel and Pol, 2010; Van Dijk et al., 2010). Besides, the rs-fMRI predictive models generated from one population could be used to predict the same cognitive ability in other populations while using different tasks (Fong et al., 2019) or tests (Rosenberg et al., 2016). These findings indicated that the predictive model generated from the brain state could be generalized to different populations. Also, the model could capture the features of a cognitive construct independent of the instrument used for operationalizing the measure.

There has been a growing interest in identifying individual neurocognitive differences by using whole-brain functional connectivity or the "connectome" approach to characterize unique patterns of brain organization for each neurocognitive function (Finn et al., 2015; Liu et al., 2018; Rosenberg et al., 2016). The application of the machine learning method further catalyzes the momentum of research to verify the feasibility and usefulness of rs-fMRI data in building models that can validly predict neurocognitive functions. A connectome-based predictive modeling (CPM) approach has been introduced to predict behavior using functional connectivity in the machine-learning framework (Shen et al., 2017). So far, CPM has been demonstrated to predict fluid intelligence (Finn et al., 2015), attention (Rosenberg et al., 2016, 2020; Wu et al., 2020), reading ability (Jangraw et al., 2018), cognitive impairment score (Lin et al., 2018), personality traits (Hsu et al., 2018) and loneliness (Feng et al., 2019).

In this study, we employed the rs-fMRI to establish a predictive model for PS for older adults. We applied the CPM approach and used whole-brain resting-state functional connectivity to predict older adults' PSs measured by the SDMT (Forn et al., 2009; Gawryluk et al., 2014). A previous rs-fMRI study revealed that a faster PS was associated with stronger functional connectivity between the left primary motor cortex and the right precentral and postcentral gyrus (Koenig et al., 2014), suggesting that connectivity strength within the motor network was positively correlated with PS performance. Furthermore, structural MRI studies found converging evidence that PS depends on processes subserved by the frontal regions and cerebellum (Böhr et al., 2007; Eckert et al., 2010; Kennedy and Raz, 2009). Task-related (Forn et al., 2009; Gawryluk et al., 2014; for review, see Silva et al., 2018) and task-demand-related activations (Forn et al., 2013) have been reported in the frontal, parietal, occipital and temporal lobes and the cerebellum. Based on these previous findings, we first hypothesized that PS could be predicted by resting-state functional connectivity in older adults. Second, we examined the characteristics of the predictive connectomes and hypothesized that it would involve the neural correlates across the whole brain (as reported in Forn et al., 2013). Third, we established the domain specificity of the model by verifying how well the model could also be applied in the same sample to predict other cognitive domains—neurocognitive abilities that are highly correlated with PS (attention: Silva et al., 2018; memory: Hedden et al., 2005; Levitt et al., 2006; Zaremba et al., 2019). Fourth, we verified the external generalizability of the model in the older participants in the Cam-CAN data set (Shafto et al., 2014; Taylor et al., 2017). Last but not least, we examined the specificity of the model by testing the model in other age groups (e.g., younger adults and middle-aged adults). The development of PS ability through the lifespan is not linear (Lee et al., 2012), and there are systematic, but not unidirectional, differences in segregation and integration across different brain regions between older and younger adults (Chong et al., 2019; Zonneveld et al., 2019). Therefore, we predicted that the model built from older adults would not be applicable to younger adults.

2. Methods

2.1. Internal validation participants

In this study, we recruited 125 right-handed older adults with no past or current neurological diseases or psychological illnesses from the local community through advertisements in public places. Participants were excluded based on the following criteria: (1) excessive head motion, as described in Section 2.4 (21 participants); (2) high score in the geriatric depression scale test (score > 8, 1 participant); (3) incomplete resting-state scanning (1 participant); and (4) incomplete cerebellum coverage of brain scanning (3 participants, see Section 2.5). Finally, 99 participants (74 females and 25 males; mean age = 66.84 years, SD = 4.59 years) remained in the prediction analysis. All participants scored above 19 in the Hong Kong version of the Montreal cognitive assessment (MoCA), indicating an absence of dementia based on the cut-off of the older Chinese adults in Hong Kong (Yeung et al., 2014). Except for the one participant who scored 20, all other participants scored equal or above 22 in MoCA, indicating that most of our participants were cognitively intact. A portion of these participants were included in a previous study (Yu et al., 2020). Written consent was obtained from all the participants prior to the study. This study was approved by the Research Ethics Committee of the University of Hong Kong.

2.2. Neurocognitive assessments

2.2.1. Processing speed

To evaluate PS, we administered the Chinese version of the SDMT (Lee et al., 2002; Smith, 1982). Participants were required to match numbers from 1 to 9 to each geometric symbol by reading aloud the number as quickly as they could in 90 s. The number of the correct matched items was recorded and was used to reflect PS ability.

2.2.2. Selective and divided attention

To evaluate selective attention ability, we administered the Arrow test (Lee et al., 2005). Participants were presented with arrows pointing either in the "up" or "down" direction in two conditions. In the "go" condition, participants were asked to identify the correct direction of the arrowheads; while in the "reverse" condition, they were asked to identify the opposite direction of the arrowheads. Each condition had four blocks with a total number of 18 trials in each block. The interference score was calculated by subtracting the reaction time (RT) in the "go" condition from the RT in the "reverse" condition, and was multiplied by -1, with a higher score indicating better selective attention. The internal consistency reliability (Cronbach's α) of the Arrow test was 0.70.

To evaluate the divided attention, we administered the Color Trails Test (CTT) with two subtests: CTT 1 and CTT 2 (Lee and Chan, 2000). In CTT 1, participants were required to connect numbers from 1 to 15 in ascending order. The even numbers were printed on yellow circles,

while the odd numbers were printed on pink circles. In CTT 2, there were two sets of numbers (1–15), with one set printed on pink circles and the other printed on yellow circles. Participants were asked to link the numbers in ascending order and alternate between pink and yellow circles. The RTs of completing the two subtests were recorded. The divided attention was assessed by subtracting the RT in CCT 1 from the RT in CCT 2 and was multiplied by -1, with a higher score indicating better divided attention. The internal consistency reliability (Cronbach's α) of the CTT was 0.77.

2.2.3. Verbal and nonverbal memory

To evaluate verbal and nonverbal memory, the Chinese Auditory Verbal Learning Test (CAVLT; Lee et al., 2002) and the Continuous Visual Memory Test (CVMT; Trahan and Larrabee, 1988) were used in the assessment. In the CAVLT, participants were presented with a list of 15 words for five trials, followed by a free-recall test of the list in each trial. The participant's verbal memory ability (total learning) was calculated by summing the number of the successfully recalled words in the five trials. In the CVMT, participants were shown 112 drawings in seven blocks. From the second block on, there were seven "old" and nine "new" stimuli in each block (42 "old" and 54 "new" in total) that participants were asked to recognize. Nonverbal memory ability (recognition) was calculated by subtracting the incorrect recognition score (false alarm) from the correct recognition score (hit).

The relationship between all the behavioral variables were assessed using the partial Pearson correlation analysis, controlling for sex, age and education. A partial Spearman correlation analysis was conducted if one of the variables did not follow a normal distribution (Kolmogorov-Smirnov Test, $p < 0.05$). The relationship between PS and age and education was explored using a bivariate Spearman correlation analysis.

2.3. Image acquisition and preprocessing

We obtained the imaging data using a 3T Philips MRI scanner at the University of Hong Kong. The resting-state fMRI data were acquired using a single-shot gradient-echo multislice echo-planar imaging (EPI) pulse sequence (slice number = 32; slice thickness = 4 mm without inter-slice gap; TR = 2000 ms; TE = 30 ms; flip angle = 90°; matrix size = 64 × 64, FOV = 230 × 230 × 128 mm³); 240 vol were acquired in about 8 min. The structural MRI data were acquired using the T1-weighted MPRAGE sequence (137 sagittal slices; slice thickness = 1.2 mm; TR = 6.64 ms; TE = 3.1 ms; flip angle = 9°; matrix size = 256 × 256, FOV = 256 × 256 × 164 mm³). The resting-state fMRI data have never been used in any previous publication.

All the images were preprocessed using SPM 12 (https://www.fil.ion.ucl.ac.uk/spm/) and DPABI 3.1 (Yan et al., 2016). For the resting-state fMRI data, the first five volumes were discarded. Images were then corrected for slice-timing and head motion. Nuisance regressors, including mean signals from white matter, cerebral-spinal fluid signals and global signals, as well as the Friston 24-motion parameters (six motion parameters, six motion derivatives and their squares), were regressed out from the data. As suggested by Power et al. (2012), volume with a mean frame-wise displacement (FD) > 0.5 mm was added as a covariate, and the one volume prior to this volume and the two volumes after this volume were also added as covariates. The number of volumes with FD > 0.5 mm ranged from 0 to 62, and the mean was 5.76 (the percentage of volumes with FD > 0.5 mm ranged from 0 to 26.4%, and the mean was 2.45%). The images were then spatially smoothed by a Gaussian kernel of 6 mm full-width-at-half-maximum (FWHM) and temporally smoothed using the frequency bandwidth of 0.01–0.1 Hz.

2.4. Head motion controls

Considering the head motion effect on the resting-state functional connectivity, participants were excluded with absolute head motion > 2 mm translation and > 2° rotation or mean FD > 0.2 mm (Jenkinson et al., 2002; Yan et al., 2013). To verify that the behavioral scores (i.e., PS, divided and selective attention, verbal and nonverbal memory) and predicted scores were not correlated with head motion, we also tested the correlation coefficients between the mean FD and the observed behavioral and predicted scores. To further control for possible head motion confounds, we also ran the identical prediction analysis with the mean FD as an additional covariate. In addition, we evaluated whether the predictive models would also be associated with the mean FD, utilizing the method in Section 2.8.

2.5. Functional connectivity network construction

Network nodes were defined using the Shen 268-node functional brain atlas that encompasses the cortex, subcortical areas and cerebellum (Shen et al., 2017). First, the functional images were normalized to the structural images, generating a deformation and an inverse deformation matrix. Following that, we warped the 268-node atlas from MNI space into individual functional space using the inverse deformation matrix. To ensure good quality of registration, the warped atlases were visually checked using SPM, and participants with poor registration were excluded (see above), resulting in 99 participant-specific atlases. We then extracted the mean time series of each node by averaging the time series of all the voxels in each node in the participant-specific atlases. The functional connectivity (edge) was calculated as the Pearson correlation coefficient (r) between the mean time series of each pair of nodes. A Fisher's r-to-z transformation was then used to normalize the correlation coefficients, and the resulting 268 × 268 matrix for each participant was utilized in the following CPM analysis.

2.6. Predictive model construction

2.6.1. Leave-one-out cross-validation

To evaluate whether the resting-state functional connectivity could be used to predict the PS in novel older adults, we applied the CPM method using a leave-one-out cross-validation (LOOCV) method (Finn et al., 2015; Rosenberg et al., 2016; Shen et al., 2017) and performed the analyses in MATLAB (R2017b, MathWorks). First, for each set of $n − 1$ participants, behavioral variables were normalized within the training set. Subsequently, the Spearman's partial correlation coefficients were calculated between the edges and the observed behavior score, controlling for sex, age and education. As suggested by Shen et al. (2017), we used the Spearman's rank correlation rather than the Pearson's correlation because the observed behavior scores in our sample did not follow a normal distribution assessed by the Kolmogorov-Smirnov Test ($p < 0.05$). Besides, because there were unequal numbers of females and males in our sample and the PS was significantly associated with age and education, we controlled for sex, age and education to select edges that were correlated with PS independent of other possible confounds. We obtained a ρ value and a p value for each edge. Next, we extracted a positive network and a negative network, respectively, by selecting edges that were positively correlated and negatively correlated with the behavior score, using a threshold of $p < 0.01$, which was adopted in previous studies (Lin et al., 2018; Rosenberg et al., 2016). We then summed the edge values in the positive and negative networks, respectively, to characterize the network strength for each participant.

Next, the network strength indices extracted from the positive and negative networks were fitted into three general linear models to generate three coefficients and three intercepts. The first one (positive network model) predicted PS with positive network scores, the second (negative network model) with negative network scores, and the third (combined network model) with the difference of the positive and negative network scores as one independent variable (positive score minus negative score; Greene et al., 2018; Rosenberg et al., 2020). The positive and negative functional connectivity indices of the left-out participant

were then fitted into these three linear models to generate three predicted scores for the left-out participants. The Spearman's correlation coefficients between the observed and predicted scores were calculated, defined as the true predictive correlation ρ_{true}. To assess the significance of the predictive connectome-based models, we adopted a permutation testing method, as the analyses in the LOOCV were not independent and the number of degrees of freedom were overestimated (Rosenberg et al., 2016). By randomly shuffling the observed behavior score, we ran the LOOCV procedure identical to the CPM analysis described above (run 5000 times). The p_{permu} value was calculated as the percentage of ρ values generated from the null-distributed samples that were larger or equal to the true predictive correlation ρ_{true}. Model performance was calculated using the fraction of explained variance (R^2, in percentage) between the predicted values and the observed values (Poldrack et al., 2019), where $R^2 = 1 - \frac{SSE}{SST}$ (SSE is the sum of squared error; SST is the sum of squared total). A negative correlation between the predicted value and actual behavior score (negative ρ value) was considered as an unsuccessful prediction and was assumed to explain none of the variance, where R^2 was set to zero.

2.6.2. Validation analysis using repeated k-fold cross-validation

To further validate our main results, we adopted repeated k-fold (i.e., 2-fold, 5-fold, and 10-fold) cross-validation methods (also called shuffle split). Taking the 2-fold cross-validation as an example, we randomly divided the participants into two subsets with approximately equal numbers (i.e., 50 and 49), with one being the training set and the other being the testing set. All the behavioral variables were normalized in the training and testing set separately. The training set was used to build a linear prediction model, and the model's parameters were further applied to predict the behavior scores of the testing set. The Spearman correlation coefficients ρ and explained variance R^2 were calculated for the positive, negative and combined network models. This procedure was repeated twice, with each subset being used as the testing set once. The two ρs and R^2 values were averaged to obtain the prediction performance. The k-fold cross-validation was further repeated 100 times, and the final prediction performance was generated from averaging all the ρ and R^2 values. The model's significance was tested using 5000 permutations.

2.7. Functional anatomy

We defined a "fast-PS network" containing edges that appeared in every iteration of the LOOCV in the positive network. In the same vein, a "slow-PS network" was defined that comprised edges that appeared in the negative network. To identify the functional anatomy of the fast- and slow-PS networks, we defined the brain nodes as different networks in two ways. The Shen 268-node functional brain atlas was classified into 10 anatomical macroscale regions (e.g., prefrontal, motor, insula; Shen et al., 2013) and eight canonical functional networks (e.g., medial frontal, frontoparietal, default mode; Finn et al., 2015). We explored the characteristics of the within- and between-network connectivity by summing the common edges using the eight functional networks in the fast- and slow-PS networks. Following this, we compared the connectivity patterns by subtracting the number of edges in the slow-PS network from the fast-PS network. Considering the eight functional networks had different numbers of nodes, we calculated and compared the proportion of the within- and between-network connectivity to control for the network size. We first summed the actual connectivity within or between the network(s) from the fast- and slow-PS network and then calculated the proportion of that connectivity (s = actual number of connectivity / total number of all possible connectivity within or between the network).

2.8. Procedures for testing the PS-CPM models

We then examined the domain specificity, the external validity and the effect of confounds of the processing speed CPM (PS-CPM) mod-

els, as described in the following sessions. The common procedures for these analyses are described below. Two network strength scores were calculated by summing the edges selected from the fast-PS network and slow-PS network. Subsequently, the fast-PS network strength, slow-PS network strength, and combination of the two network strengths (fast-PS network strength minus slow-PS network strength) were fitted into three linear models separately (fast-PS network model, slow-PS network model, combined network model). The estimated model parameters from the above three linear models were applied to the other dependent variables of our primary data set and the external data set respectively. For testing the PS-CPM model on the external data sets, the network strengths were calculated with the same procedure, and evaluated against the corresponding dependent variables. A Spearman correlation analysis was then conducted between the predicted scores and the observed behavioral scores, as some of the variables did not follow a normal distribution (Kolmogorov-Smirnov Test, $p < 0.05$). An R^2 value was also computed to evaluate the prediction performance. Permutation testing (5000 times) was adopted to test the significance of the prediction.

2.9. Domain specificity of the PS-CPM models

In order to investigate the domain specificity of the PS-CPM models, we tested if the models also predicted attention and memory performance, using the method in Section 2.8. We generated three predicted scores. To explore whether the prediction was driven by the correlation between PS and attention/memory, we also tested the partial Spearman correlation between the predicted scores and the observed scores, while controlling for PS. To further explore the effect of attention and memory on our PS-CPM models, we additionally controlled attention and memory in the edge selection and tested whether it would affect the prediction performance of PS-CPM models on PS. To explore whether the PS-CPM models could predict cognitive function that was not associated with PS, we also tested the predictive value of the models on the total move scores of Tower of London (ToL) (for details, see Supplementary Materials). The total number of move in the ToL task was found not to be correlated with PS, and it mainly assesses planning process (Riccio et al., 2004). The false discovery rate (FDR) procedure was further applied to the number of comparisons. Statistical significance was considered to be $p < 0.05$, two-tailed. To investigate the specificity of the PS-CPM models, we also used Hotelling-Williams t-test (Steiger, 1980) to test whether the correlations between the network strengths (fast-PS and slow-PS networks) and PS were significantly different from the correlation between the network strengths and (1) attention and (2) memory.

2.10. External validation: Cam-CAN data set

2.10.1. Participants

We used an open data set of participants from Stage 2 of the Cambridge center for Ageing and Neuroscience (Cam-CAN) project (available at http://www.mrc-cbu.cam.ac.uk/datasets/camcan/; details about this project can be found in previous work (Shafto et al., 2014; Taylor et al., 2017). A list of publications using this data set could be found at: https://www.cam-can.org/index.php?content=publications. Participants in the external validation were selected from a total of 708 participants with demographic information (e.g., age, sex, education) available. Participants were included according to the following criteria: (1) right-handed (73 participants excluded); (2) with all MRI modality data available (e.g., resting-state fMRI, structural MRI; 60 participants excluded); (3) head motion < 2 mm translation and < 2° rotation, mean frame-wise displacement (FD) < 0.2 mm (Jenkinson et al., 2002; Yan et al., 2013; 203 participants excluded); (4) Good registration quality (16 participants excluded); (5) complete brain scanning (with no missing brain nodes; 25 participants excluded); and (6) with a behavior score of the processing speed task (choice response time task, see Section 2.9.2) available and an accuracy > 75% (36 participants excluded).

Finally, we included 295 participants with the Mini-mental State Examination (MMSE; Folstein et al., 1975) scores above 24 in the external validation analyses. The participants were further divided into three groups: 101 younger adults (50 females and 51 males; mean age = 30.65 years, SD = 5.12 years), 103 middle-aged adults (53 females and 50 males; mean age = 48.65 years, SD = 5.71 years) and 91 older adults (44 females and 47 males; mean age = 72.09 years, SD = 7.63 years).

2.10.2. Processing speed measurement

The choice response time task (CRT) was used to assess the PS in the new sample. The CRT required participants to make appropriate responses based on the presented stimuli. It has been suggested that the CRT and SDMT measure a similar construct, and the performance of these two tests are associated (Deary et al., 2011; Iverson et al., 2005). In the CRT, participants were presented with an image of a hand with four blank circles above each finger and were asked to place their right hands on a response box with four fingers on four separate buttons. In each trial, one of the four blank circles above the hand would turn black, and participants had to press the button using the corresponding finger as quickly as possible (maximum 3-second response time). The inter-trial intervals (ITI) varied pseudo-randomly with a positively skewed distribution and a mean of 3.7 s, from a minimum of 1.8 to a maximum of 6.8 s. There were 67 trials in total. The mean reaction times (RT) from the stimulus onset to pressing the button were recorded and reflected the PSs of the participants. The RT was multiplied by −1 and z-transformed before being entered into the following analysis, with a higher score representing faster PS. The internal consistency reliability (Cronbach's α) of the CRT was 0.97.

2.10.3. Image parameters and preprocessing

The MRI data were collected at the Medical Research Council Cognition and Brain Science Unit (MRC–CBSU) on a 3T Siemens TIM Trio System, with a 32-channel head coil. The resting-state fMRI data were acquired using a gradient- echo-planar imaging (EPI) sequence (slice number = 32 in descending order; slice thickness = 3.7 mm with an interslice gap of 20%; TR = 1970 ms; TE = 30 ms; flip angle = 78°; matrix size = 64 × 64, FOV = 192 × 192 × 142 mm^3); 261 vol were acquired in about 8 min and 40 s. The structural MRI data were acquired using a T1-weighted MPRAGE sequence (192 sagittal slices; slice thickness = 1.2 mm; TR = 2250 ms; TE = 2.99 ms; flip angle = 9°; matrix size = 256 × 240, FOV = 256 × 240 × 192 mm^3).

All the images were preprocessed as described in Section 2.3. The number of volumes with FD > 0.5 mm ranged from 0 to 63, and the mean was 9.92 (the percentage of volumes with FD > 0.5 mm ranged from 0 to 24.6%, and the mean was 3.9%). Participants were excluded with absolute head motion > 2 mm translation and > 2° rotation or mean FD > 0.2 mm. The performance (mean RT) of CRT was not significantly correlated with mean FD (younger adults: $\rho = 0.045$; $p = 0.66$; middle-aged adults: $\rho = 0.028$; $p = 0.78$; older adults: $\rho = 0.13$; $p = 0.23$), suggesting that head motion was not a significant potential confound of our validation results.

2.10.4. Functional connectivity network construction

All procedures of constructing resting-state networks were the same as those described in Section 2.5.

2.10.5. CPM prediction

To verify if the identified PS-CPM models could be generalized to the older adults, we applied the approach in Section 2.8. We fitted the network strengths of the Cam-CAN data set to the three linear models (fast-PS network model, slow-PS network model, combined network model) and generated three predicted scores for PS. To control for the head motion effect, we also calculated the partial Spearman correlation coefficients between the predicted scores and CRT scores by adding the mean FD as a covariate. The Spearman correlation test was used because the CRT scores did not follow a normal distribution (Kolmogorov-Smirnov test, $p < 0.05$).

2.10.6. PS-CPM validated in other age groups in the Cam-CAN data set

To investigate the specificity of the PS-CPM models, we repeated our external validation analyses in the younger-aged group and in the middle-aged group, using the Cam-CAN data set. The other analyses were identical to those in the aged group for the younger and middle-aged groups.

2.11. Supplementary analyses

Four supplementary analyses were conducted to evaluate the influence of potential confounds on our results. For clarity, the primary CPM model described in Section 2.6.1 is labelled as C1 (stands for CPM model 1). In the analysis of C1, C2, C4 and C5, partial correlation was applied in the edge selection loops, and the corresponding variables were entered into the partial correlation function as nuisance variables. We examined the effect of head motion in model C2 by entering mean FD, age, sex and education as nuisance covariates (also described in Section 2.4). As PS was highly correlated with age, how and whether to control age could potentially influence the CPM results. Thus, we also used different covariate controlling methods. In C3, we controlled for nuisance variables by regressing out the age, sex and education from both behavioral and connectivity measures of the training set in each loop and utilized simple correlation in the edge selection. In C4, we controlled only for sex and education to explore the effect of age on the PS-CPM model.

Lastly, we also explored the effect of the p threshold selection in the edge selection in model C5. Instead of a predefined p-value, we tested a range of p values from 0.001 to 0.1 with an interval of 0.001 (Gao et al., 2019; Jiang et al., 2018). Optimal p thresholds that led to the best prediction performance were obtained for the positive network ($p = 0.093$) and negative network ($p = 0.013$) separately (C5; for details, see Supplementary Materials). In the supplementary analyses (C2-C5), different CPM models were constructed and generalized to the younger, middle-aged, and older adults in the Cam-CAN data set. To further investigate whether the predictions of different supplementary analyses were significantly different from those of C1, we applied the Hotelling-Williams t-test (Steiger, 1980) and compared the significant correlation coefficients in the internal and external validations.

3. Results

3.1. Connectivity–behavior prediction

The demographic information of the 99 participants is shown in Table 1. The connectome-based predictive models significantly predicted the PS scores of the novel participants (left-out participant in the LOOCV) using resting-state functional connectivity (positive network: $\rho = 0.36$, $R^2 = 8.58\%$, $p_{permu} = 0.010$; negative network: $\rho = 0.42$, $R^2 = 11.20\%$, $p_{permu} = 0.003$; combined network: $\rho = 0.40$, $R^2 = 10.49\%$, $p_{permu} = 0.001$; Fig. 1A). Furthermore, the models remained significant ($ps_{permu} < 0.05$) after applying different k-fold cross-validation schemes (Table 2). For the positive network, the number of edges extracted from each iteration ranged from 496 to 654, and the fast-PS network contained 331 common edges (0.93% of the 35,778 total edges) occurring in every iteration. For the negative network, the number of edges extracted from each iteration ranged from 527 to 708, and the slow-PS network contained 380 common edges (1.06% of the total edges). The fast-PS and slow-PS networks are separately shown in Fig. 2.

3.2. Functional network anatomy

We identified connectivity patterns within and between the eight networks in the fast-PS network and the slow-PS network, after taking the eight functional network sizes into consideration and obtaining the proportion of each network (Fig. 3). Our results showed that, in the fast-PS network, connectivity within the motor network contributed the

Table 1

Demographic information of the participants used in this study and correlations between the studied variables, controlling for sex, age and education. The correlation analyses were conducted on the z-transformed values of the variables.

Variables	Mean	SD	Correlation coefficients (r or ρ)						
			Processing speed	Selective attention	Divided attention	Verbal memory	Nonverbal memory	Fast-PS	Slow-PS
Our sample: N = 99									
1. Sex (Female/male)	74/25								
2. Age (years old)	66.84	4.59	−0.55***[a]	-.17[a]	−0.29**[a]	−0.39***[a]	-.19[a]		
3. Education (years)	12.02	4.65	.35***[a]	.17[a]	.18[a]	.41***[a]	-.002[a]		
4. Processing speed[1] (n)	53.74	10.47	—						
5. Selective attention (ms)	−12.54	5.89	.21*	—					
6. Divided attention (ms)	−52.26	24.95	.23**	.31***	—				
7. Verbal memory (n)	47	9.45	.35***	.08	.002[b]	—			
8. Nonverbal memory (n)	71	7.15	.32**	.17	.10[b]	.17[b]	—		
9. Fast-PS network strength	39.41	32.06	.74***	.23*[c]	.33**[c]	.31**[c]	.32**[c]	—	
10. Slow-PS network strength	−28.74	37.71	−0.69***	−0.24*[c]	−0.29*[c]	−0.30**[c]	−0.34**[c]	−0.92***	—
Cam-CAN sample: N = 91									
1. Sex (Female/male)	44/47								
2. Age (years old)	72.09	7.63	−0.34**[a]						
3. Education (years)	19.45	4.16	-.16[a]						
4. Processing speed[2] (ms)	−692.60	145.03	—						

Note: Fast-PS and slow-PS network strengths are extracted from the PS-CPM models that appeared in every internal validation loop. The correlations between the network strengths and PS only indicate the relationship between PS-CPM networks and PS, while the prediction results (ρ, R^2 and p_{permu}) of the PS-CPM models are shown in Fig. 1A. N, number of participants; M, mean; SD, standard deviation; Processing speed[1]: Symbol Digit Modalities Test; Processing speed[2]: Choice Response Task; Selective attention: Arrow test; Divided attention: Color Trail Test; Verbal memory: Chinese Auditory Verbal Learning Test; Nonverbal memory: Continuous Visual Memory Test. Unless otherwise specified, the correlation coefficients were acquired using Partial Spearman correlation analysis. [a]: bivariate Spearman correlation coefficients.

[b] Partial Pearson's correlation coefficients.

[c] : p-values are obtained based on FDR corrections; * $p < 0.05$, ** $p < 0.01$, *** $p < 0.001$.

A   PS-CPM internal validation prediction
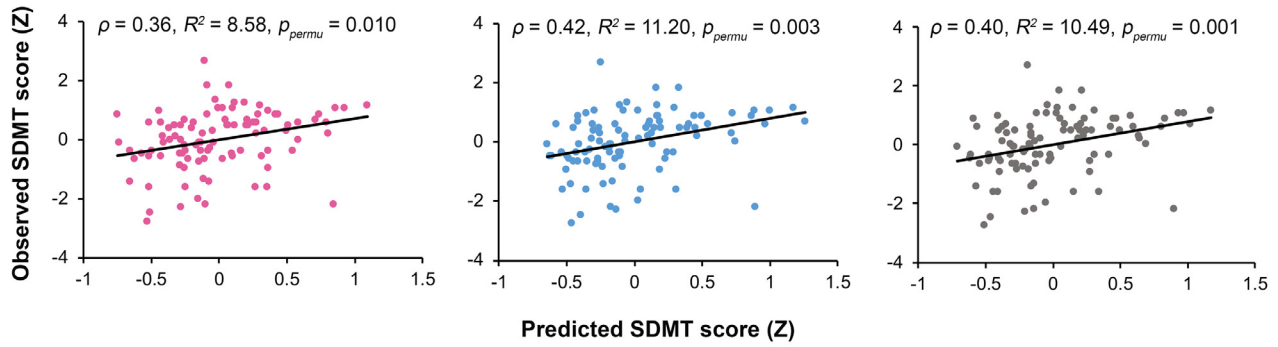
B   PS-CPM External validation prediction in Cam-CAN older adults

● Fast-PS network model   ● Slow-PS network model   ● Combined network model
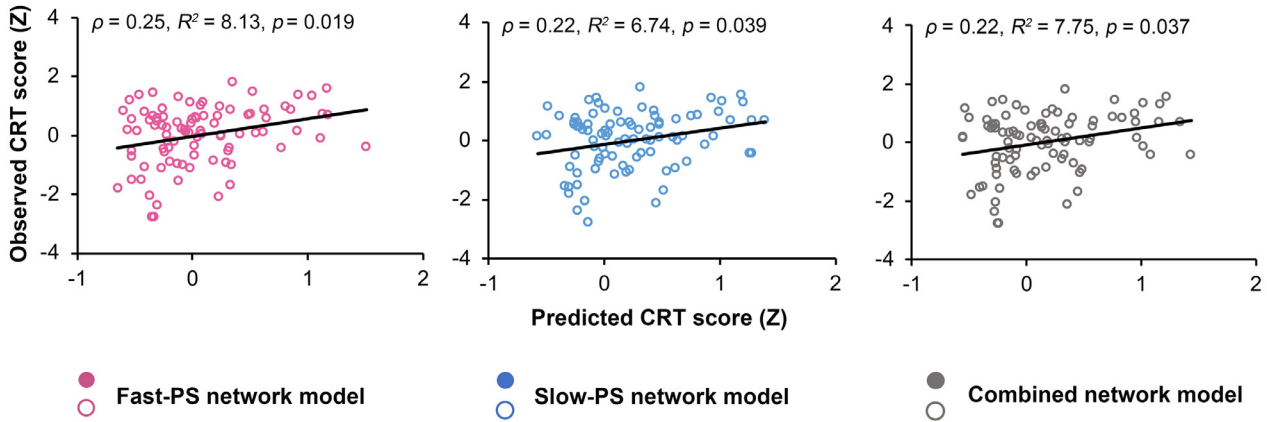○   ○   ○

Fig. 1. Resting-state functional connectivity predicts processing speed (SDMT score) of older adults in the internal validation data set (A) and predicts processing speed (CRT score) of older adults in the external validation data set (B). Behavioral scores were standardized for visualization. PS: processing speed; SDMT: Symbol Digit Modalities Test; CRT: Choice Response Task. p_{permu}: p-value obtained from permutation tests (5000 times).

Table 2
K-fold cross-validation results of CPM analyses.

k-fold	Positive network					Negative network					Combined network				
	ρ		R^2 (%)			ρ		R^2 (%)			ρ		R^2 (%)		
	mean	SD	mean	SD	p_{permu}	mean	SD	mean	SD	p_{permu}	mean	SD	mean	SD	p_{permu}
2-fold	0.36	0.05	10.34	2.75	< 0.001	0.38	0.06	10.76	2.80	0.001	0.39	0.05	11.36	2.66	< 0.001
5-fold	0.36	0.05	14.22	2.77	0.003	0.40	0.05	15.33	2.93	< 0.001	0.39	0.04	15.19	2.50	0.0014
10-fold	0.35	0.05	19.09	3.24	0.005	0.40	0.05	21.00	3.46	0.002	0.38	0.05	20.78	3.94	0.0016

Note: *SD*: standard deviation; p_{permu}: p values obtained from permutation (5000 times).

Fast-PS network   **Slow-PS network**

Prefrontal
Motor
Insula
Parietal
Temporal
Occipital
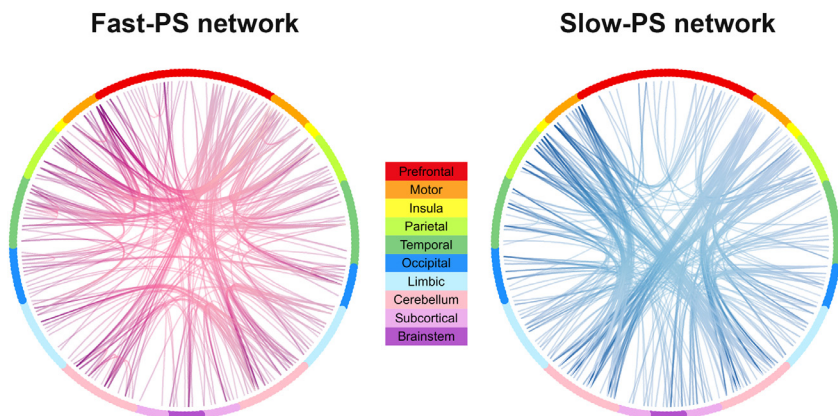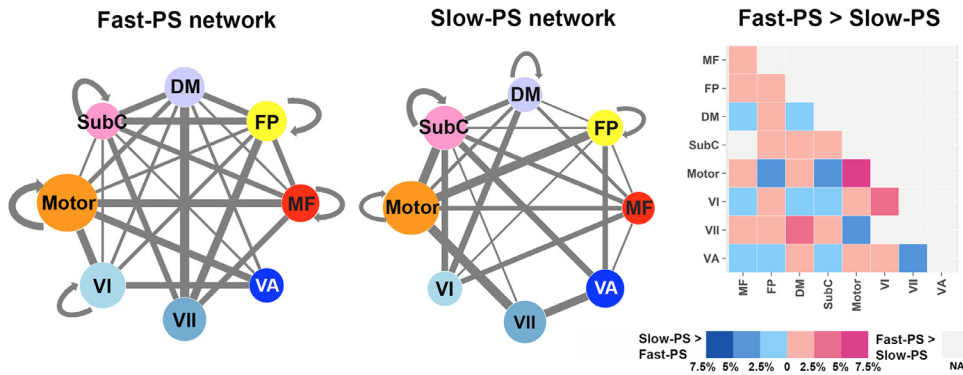Limbic
Cerebellum
Subcortical
Brainstem

Fig. 2. Fast-PS network (left, pink) and slow-PS network (right, blue) obtained from the PS-CPM models and distributed in macroscale brain regions. The demonstrated edges are the common edges that occurred in every iteration of the CPM construction. There are 331 common edges in the fast-PS network and 380 common edges in the slow-PS network. The 10 macroscale regions include the prefrontal cortex, motor cortex, insula, parietal cortex, temporal cortex, occipital cortex, limbic (including the cingulate cortex, amygdala and hippocampus), cerebellum, subcortical areas (thalamus and striatum) and brainstem. Connectivity figures were created using ggraph (CRAN.R-project.org/package=ggraph) . (For interpretation of the references to colour in this figure legend, the reader is referred to the web version of this article.)

Fast-PS network and Slow-PS network (control for network size)

Fig. 3. Fast- and slow-PS networks and their comparison in canonical functional networks. Each node represents one functional network. Larger circles and thicker lines represent a greater proportion of connections. Each cell (fast-PS > slow-PS) represents the comparison of edges within and between each functional network. The connectivity within and between each functional network was obtained by extracting the proportion of that connectivity (actual number of connectivity / total number of all possible connectivity within or between the network(s)), controlling for network size. The proportions ranged from 3.0% to 13.5% for the functional networks in the fast-PS network, and from 2.7% to 12.5% for the functional networks in the slow-PS network. PS: processing speed; MF: medial frontal; FP: frontoparietal;

DM: default mode; SubC: subcortical and cerebellum; VI: visual I; VII: visual II; VA: visual association.

most, whereas in the slow-PS network, connectivity between the motor-visual II, motor-SubC and motor-frontoparietal networks contributed the most. The comparison between the two networks (*fast-PS > slow-PS*) showed that the fast-PS network consisted of more within-network connectivity in the motor and visual I networks, while the slow-PS network consisted of more between-network connectivity in the motor-visual II, motor-SubC and motor-frontoparietal networks.

These results demonstrated that more within-network connectivity in the motor and visual network indicated faster PSs, whereas more between-network connectivity in the motor-visual, motor-SubC and motor-frontoparietal networks indicated slower PSs.

3.3. Motion control

Head motion, referring to the mean FD, was not significantly associated with the PS ($\rho = 0.08$, $p = 0.39$), attention (Arrow: $\rho = 0.11$, $p = 0.27$; CTT: $\rho = 0.14$, $p = 0.16$) or memory (CAVLT: $\rho = 0.06$, $p = 0.58$; CVMT: $\rho = -0.03$, $p = 0.81$). Neither the predicted PS score generated by the positive network ($\rho = -0.06$, $p = 0.55$) nor the negative network ($\rho = 0.07$, $p = 0.48$) was correlated with the mean FD. In addition, our PS-CPM models did not significantly predict head motion (fast-PS network: $\rho = 0.01$, $R^2 = 0.02\%$, $p_{permu} = 0.47$; slow-PS network: $\rho = 0.09$, $R^2 = 1.49\%$, $p_{permu} = 0.20$; combined network: $\rho = 0.05$, $R^2 = 0.55\%$, $p_{permu} = 0.31$). Furthermore, the PS-CPM models remained significant after adding the mean FD as an additional covariate (positive network: $\rho = 0.36$, $R^2 = 8.66\%$, $p_{permu} = 0.009$; negative network: $\rho = 0.42$, $R^2 = 10.94\%$, $p_{permu} = 0.002$; combined network: $\rho = 0.41$, $R^2 = 10.38\%$, $p_{permu} = 0.001$). The common edges were highly overlapped with the main results after controlling for motion (percentage of overlapping: fast-PS network: 94.12%; slow-PS network: 95.73%). These results suggested that head motion did not have significant confounding effects on our major findings.

3.4. Domain specificity

The associations between each behavioral variable are shown in Table 1. PS was negatively associated with age. Our behavioral exploratory analyses confirmed that PS was positively correlated with selective (arrow test) and divided (CTT) attention and verbal (CAVLT) and nonverbal (CVMT) memory, and was not correlated with planning function (ToL). Our results showed that the PS-CPM models (fast-PS network, slow-PS network and combined network) significantly predicted attention and memory following FDR correction ($\rho s > 0.22$, $Rs^2 > 4.26\%$, $ps < 0.05$) (Table 3). However, the predictions were not significant after controlling for PS ($|\rho s| < 0.19$, $Rs^2 < 3.30\%$, $ps > 0.27$). These results suggested that the associations between PS-CPM models and atten-

tion/memory were largely driven by the association between PS and attention/memory in older adults. On the other hand, the PS-CPM models still significantly predicted PS after controlling for attention and memory (positive network: $\rho = 0.40$, $R^2 = 10.25\%$, $p_{permu} = 0.004$; negative network: $\rho = 0.31$, $R^2 = 5.98\%$, $p_{permu} = 0.031$; combined network: $\rho = 0.37$, $R^2 = 8.30\%$, $p_{permu} = 0.005$). Furthermore, Hotelling-Williams t-tests showed that the correlations between the network strengths and PS were significantly larger than the correlations between network strengths and attention/memory measures (attention: $|ts| > 3.14$, $ps < 0.001$; memory: $|ts| > 2.79$, $ps < 0.01$). Besides, the PS-CPM models did not significantly predict planning function. The above results might suggest that the common networks derived from the PS-CPM models mainly captured the construct of PS. In sum, our results showed the PS-CPM models, which mainly captured the feature of PS, could be used for predicting selective and divided attention, as well as verbal and nonverbal memory in the same sample.

3.5. External validation: cam-can data set

The demographic information of the Cam-CAN participants is shown in Table 1 and Table 4. The internal and external validation samples (older adults) differed significantly in sex ($\chi^2 = 14.04$, $p < 0.001$), age ($t = -5.80$, $p < 0.001$) and education ($t = -11.57$, $p < 0.001$). The fast- and slow-PS networks significantly predicted the mean RT of the CRT in older adults in the Cam-CAN sample (fast-PS network: $\rho = 0.25$, $R^2 = 8.13\%$, $p = 0.02$; slow-PS network: $\rho = 0.22$, $R^2 = 6.74\%$, $p = 0.04$; combined network: $\rho = 0.22$, $R^2 = 7.75\%$, $p = 0.04$; Fig. 1B). However, our PS-CPM models could not be generalized to either the younger adults (fast-PS network: $\rho = 0.01$, $R^2 = 0.14\%$, $p = 0.92$; slow-PS network: $\rho = 0.04$, $R^2 = 0.60\%$, $p = 0.66$; combined network: $\rho = 0.04$, $R^2 = 0.39\%$, $p = 0.72$) or the middle-aged adults (fast-PS network: $\rho = 0.01$, $R^2 = 0.24\%$, $p = 0.93$; slow-PS network: $\rho = -0.05$, $R^2 = 0$, $p = 0.60$; combined network: $\rho = -0.03$, $R^2 = 0$, $p = 0.77$), which confirmed our *a priori* hypotheses. These findings remained unchanged after controlling and adding the mean FD as a covariate, indicating that head motion did not significantly influence our results. Details of the results are shown in Table 4. Our results suggested that the PS-CPM models generated from our own sample could be generalized to predict the PS ability in older adults but could not be generalized in the younger adults or middle-aged adults.

To further investigate why the PS-CPM models could not be generalized to the younger groups, we did several exploratory analyses (for details, see Supplementary Materials). First, we used resting-state functional connectivity and tried to build internal validation CPM models in the younger and middle-aged groups from the Cam-CAN data set. Results showed that we could not obtain CPM models that signifi-

Table 3
PS-CPM models predict other cognitive functions.

Neurocognitive Assessments	Fast-PS network				Slow-PS network				Combined network			
	ρ	R^2 (%)	p_{permu}	p_{corr}	ρ	R^2 (%)	p_{permu}	p_{corr}	ρ	R^2 (%)	p_{permu}	p_{corr}
Selective attention (Arrow)	**0.22**	**6.35**	**0.010**	**0.012**	**0.24**	**7.98**	**0.007**	**0.010**	**0.25**	**7.49**	**0.006**	**0.010**
Divided attention (CTT)	**0.32**	**7.81**	**0.001**	**0.002**	**0.31**	**6.15**	**0.001**	**0.003**	**0.33**	**7.15**	**<0.001**	**0.002**
Verbal memory (CAVLT)	**0.25**	**4.26**	**0.005**	**0.009**	**0.30**	**5.73**	**0.002**	**0.003**	**0.29**	**5.22**	**0.003**	**0.007**
Nonverbal memory (CVMT)	**0.33**	**10.19**	**<0.001**	**0.001**	**0.36**	**12.06**	**<0.001**	**0.001**	**0.35**	**11.61**	**<0.001**	**0.001**
Planning function (ToL)	0.03	1.28	0.382	0.382	0.08	2.24	0.219	0.253	0.06	1.83	0.289	0.382
controlling for PS												
Selective attention (Arrow)	0.08	1.60	0.220	0.354	0.10	2.80	0.157	0.294	0.10	2.33	0.147	0.354
Divided attention (CTT)	0.13	0.76	0.086	0.268	0.11	0.30	0.130	0.294	0.13	0.51	0.085	0.268
Verbal memory (CAVLT)	−0.13	1.29	0.891	0.891	−0.06	0.29	0.730	0.843	−0.10	0.69	0.836	0.891
Nonverbal memory (CVMT)	0.14	1.91	0.089	0.268	0.19	3.30	0.034	0.268	0.16	2.76	0.063	0.268
Planning function (ToL)	0.02	0.43	0.440	0.550	0.08	1.19	0.236	0.354	0.05	0.84	0.314	0.550

Note: PS-CPM: processing speed connectome-based modeling; Arrow: Arrow test; CTT: Color Trail Test; CAVLT: Chinese Auditory Verbal Learning Test; CVMT: Continuous Visual Memory Test; ToL: Tower of London. Numbers in bold indicate significant correlations after FDR correction ($p < 0.05$).

Table 4
External validation in the Cam-CAN data set.

	Younger adults $N = 101$		Middle-aged adults $N = 103$		Older adults $N = 91$	
	Mean	SD	Mean	SD	Mean	SD
Sex (Female/male)	50/51		53/50		44/47	
Age (years old)	30.65	5.12	48.65	5.71	72.09	7.63
Education (years)	21.95	3.2	20.04	3.16	19.45	4.16
Processing speed (ms)	−474.9	71.6	−548.8	80.3	−692.6	145.03
Pearson correlation (PS and age)	−0.105		**−0.217***		**−0.322***	

PS-CPM models	Fast-PS	Slow-PS	Combined	Fast-PS	Slow-PS	Combined	Fast-PS	Slow-PS	Combined
External validation (R^2)	0.14%	0.60%	0.39%	0.24%	0.00%	0.00%	**8.13%***	**6.74%***	**7.75%***
Control for FD (R^2)	0.14%	0.59%	0.38%	0.22%	0.00%	0.00%	**7.90%***	**6.58%***	**7.55%***

Note: ρ indicated Spearman correlation coefficients; SD: Standard deviation; PS: Processing speed; FD: frame-to-frame displacement head motion; Numbers in bold indicate significant results ($p < 0.05$); *: $p < 0.05$.

cantly predicted the PS of the younger or middle-aged adults. Second, we tested whether the variance of PS in the younger groups was significantly different from the variance in the older adults of the Cam-CAN data set. Results showed that older adults had significantly higher CRT variance, compared to the younger and middle-aged adults. Third, we compared our PS-CPM networks (fast-PS network and slow-PS network) with the SA-CPM (sustained attention-CPM, high-attention network and low-attention network) networks derived from younger adults in Rosenberg et al. (2016). Results showed that the overlaps between the fast-PS and high-attention network (percentage of overlapping: 0.18%), and between the slow-PS and low-attention network (percentage of overlapping: 0%) were very low.

3.6. Supplementary analyses

The results of the supplementary analyses are shown in Fig. 4 (for details, see Supplementary Table S1 and S2). In the internal validation, our results showed that in different supplementary analyses, the resting-state CPM models still significantly predicted PS (positive network: $R^2 = 8.58 \sim 11.70\%$; negative network: $R^2 = 5.98 \sim 12.25\%$; combined network: $R^2 = 10.38 \sim 12.40\%$; all $ps_{permu} < 0.05$). In the external validation in the older adults, the PS-CPM models remained significant to predict the PS (fast-PS network: $R^2 = 8.13 \sim 9.64\%$; slow-PS network: $R^2 = 6.53 \sim 7.66\%$; combined network: $R^2 = 7.75 \sim 9.13\%$;

all $ps < 0.05$). For external validation in the younger and middle-aged adults, all the supplementary analyses showed that the PS-CPM models could not be generalized to predict the PS in these two groups (fast-PS network: $R^2 = 0 \sim 0.29\%$; slow-PS network: $R^2 = 0 \sim 0.91\%$; combined network: $R^2 = 0 \sim 0.58\%$; all $ps > 0.05$).

Overall, it was observed that the CPM model predictions in the supplementary analyses were not markedly different from those of the initial model, particularly during external validation, which suggested that our core findings were robust across different control analyses.

4. Discussion

This study's findings indicated that, by using the data-driven CPM method, the resting-state functional connectivity could significantly predict PS in older adults. The predictive networks incorporated functional connectivity among the frontal, parietal, temporal and occipital regions and the cerebellum, which belongs to the motor, frontoparietal, medial frontal, default-mode, visual-related and SubC networks, respectively. We further identified two connectome patterns (fast- and slow-PS networks) associated with PS at the region and network levels. Specifically, the fast-PS network consisted of largely within-network connectivity in the motor and visual networks. The slow-PS network, on the other hand, consisted of largely between-network connectivity in the motor-SubC and motor-frontoparietal networks. Our findings also con-

A Prediction performance in internal validation (older adults)
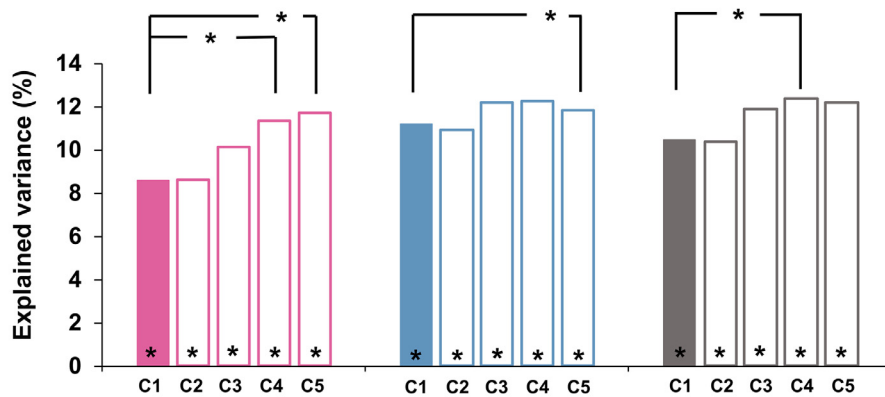
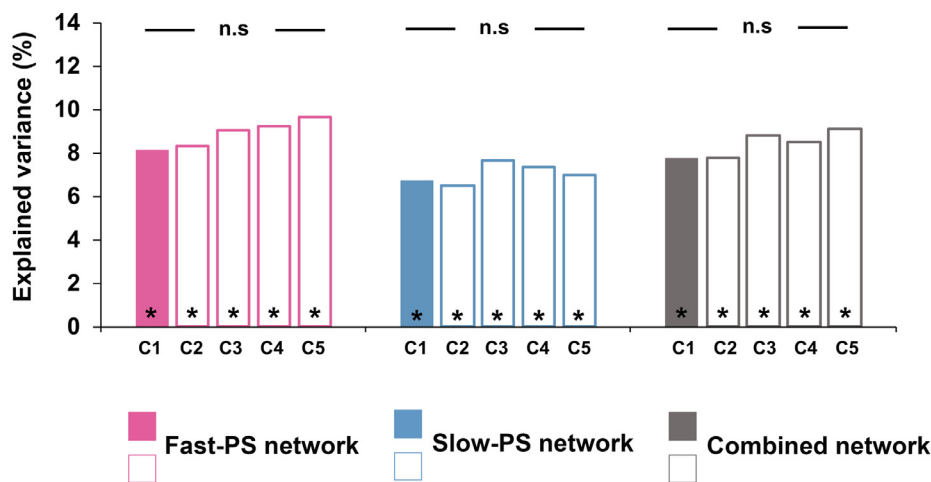## B Prediction performance in external validation (older adults)

Fig. 4. Prediction performance (explained variance) of different supplementary analyses in older adults in the internal (A) and external (B) validation. C1: main CPM analyses (controlling for age, sex and education in edge selection); C2: effect of head motion (controlling for age, sex, education and mean FD in edge selection); C3: effect of regression methods of possible confounds (for each set of n-1 participants, regressing out age, sex and education from the functional connectivity matrix and PS score before training the CPM models); C4: effect of age (controlling for sex and education in edge selection); C5: effect of p threshold selection (optimal p thresholds for the positive network ($p = 0.093$) and negative network ($p = 0.013$) separately). "—*—" indicates the comparisons between the correlation coefficient of C1 and the correlation coefficients of other supplementary analyses are significant. "—n.s.—" indicates the comparisons between the correlation coefficient of C1 and the correlation coefficients of other supplementary analyses (C2-C5) are not significant. "*" indicates $p < 0.05$.

firmed our *a priori* expectation that the PS-CPM models could also predict attention and memory in the internal validation sample. Models identified from our sample could predict the PS ability of participants in an external independent sample of older adults but not in samples of younger adults or middle-aged adults, showing that our predictive models were robust, generalizable and specific to the older adults. Our study provides promising evidence that resting-state functional connectivity across multiple regions can be used to identify individual differences in PS in older adults.

4.1. Age specificity of PS-CPM network

In this study, we have successfully demonstrated that the whole-brain resting-state functional connectivity data could predict PS in older adults using the CPM method. Resting-state functional connectivity has been consistently recognized as quite well-suited for clinical applications, as it can be obtained from populations who have difficulty performing tasks within a short period (Fox and Greicius, 2010). In addition, the scanning protocol for resting-state fMRI is relatively standard, which promotes the generalizability of the predictive models in other big data sets (Smith et al., 2013). Besides, a large body of literature has shown its predictive ability in different functions (Arnemann et al., 2015; Liu et al., 2018; Ramos-Nuñez et al., 2017; Siegel et al., 2016). Given that abnormal changes in the brain took place years before the clinical symptoms occurred in the neurodegenerative disorders (Pievani et al., 2014; Villemagne et al., 2013), rs-

fMRI seems like an attractive neuromarker for clinical prognoses. Besides, external validation analyses revealed that our PS-CPM models could be generalized to predict PS in an independent sample of older adults, indicating that our predictive models were relatively robust. Taken together, our findings suggest these age-related neuromarkers might complement conventional assessments and yield potential clinical benefits.

On the other hand, CPM models generated from older adults could not be generalized to younger and middle-aged adults. There are several possible reasons. First, the variance in the older adults of the Cam-CAN data set was significantly larger than the variance in the younger and middle-aged groups. Besides, we could not find internally validated CPM models that could predict the CRT score in these two groups. These findings could suggest that the resting-state functional connectivity might not be able to capture the small individual variability of the processing speed as assessed by the CRT in the younger and middle-aged adults. Second, our internal validation data set only included older adults. Thus, only a limited range of PS scores were trained in the model construction, which might explain why the model could not capture the cognitive characteristics outside the included range. Future work could build PS-CPM models on samples with more diverse age and behavioral score ranges, and test their generalizability across different age groups. Third, the PS-CPM networks were not similar to the SA-CPM networks derived from younger adults (Rosenberg et al., 2016). This might suggest that our PS-CPM primarily captured the neurocognitive function variance in older adults.

4.2. Domain specificity of PS-CPM network

We observed that the PS-CPM models could also predict attention and memory in the same sample with which we had worked. On the other hand, our exploratory analysis confirmed that the prediction was largely driven by the association between the PS and attention/memory. Besides, the PS-CPM models could still predict PS even after controlling for attention/memory. These results suggested that our model was also predictive of memory and attention functions, which was likely to be due to their shared processes with processing speed, since their associations disappeared after controlling for processing speed. On the contrary, our model was likely to capture relatively unique cognitive processes of processing speed, given the predictivity was maintained even after controlling for attention and memory. Therefore, the PS-CPM model should be applied to primarily predict processing speed, and its predictivity on other cognitive functions may be bound by common processes shared by those functions with processing speed.

Previous studies have demonstrated that attentional CPM models can predict other cognitive functions, such as inhibition control (Fountain-Zaragoza et al., 2019) and memory recall (Jangraw et al., 2018). These findings suggest that the predictive CPM networks of a certain neurocognitive ability might be useful for predicting other related neurocognitive abilities. The PS theory of aging suggests that PS is the leading predictor of changes in cognitive abilities, especially in fluid abilities (Salthouse, 1996). Accumulated evidence supports that PS is associated with attentional deficits (Forn et al., 2013; Silva et al., 2018, 2019) and predicts memory performance (Brébion et al., 2000; Finkel et al., 2007; Hedden et al., 2005; Levitt et al., 2006; Zaremba et al., 2019). Our study not only confirmed that PS had a close relationship with attention and memory but also revealed that functional connectivity models predicting PS could provide useful information about attention and memory performance. Based on the general slowing theory, aging is accompanied by a general reduction in PS that in turn leads to deterioration in cognitive functions such as attention and memory performance (Finkel et al., 2007; Luo and Craik, 2008; Salthouse, 1996). Our findings could suggest that declines in attention and memory functions might be caused by the alteration in the overlapping neural systems between the PS and these cognitive functions. Research has indicated that the frontoparietal, motor and cerebellum networks are involved in attention processes (Bush, 2011) and recognition memory (Meyer and Damasio, 2009). In line with these findings, our PS-CPM networks, encompassing the frontal and parietal regions as well as the cerebellum, appear to be applicable for predicting attention and memory. Future work could test the specificity and generalizability of the PS-CPM models in other PS and cognitive tests.

4.3. Connectome patterns of the fast- and slow-PS networks

The fast- and slow-PS networks generated from the CPM revealed that functional connectivity across multiple neural systems (i.e., the motor, SubC, frontoparietal, medial frontal, default-mode and visual-related networks) could be used to predict PS in older adults. A large amount of literature has investigated the age-related changes in these neural networks and their relationships with PS (Eckert, 2011; Ferreira and Busatto, 2013). Resting-state study found that increased connections within the motor network was associated with better SDMT performance (Koenig et al., 2014). Normal aging might disrupt the function of the motor network, which could affect the preparation and planning of movements and result in longer reaction times (Wu et al., 2007). Structural declines in the frontal lobe and the cerebellum were thought to contribute to age-related decline in PS (Eckert et al., 2010; Lu et al., 2013). The default-mode network has consistently been shown to decrease in network connectivity through the aging process, resulting in general cognitive decline (Hafkemeijer et al., 2012; Hohenfeld et al., 2018; Prvulovic et al., 2011). The visual network, along with other attention networks, becomes less cohesive across the human lifespan (Betzel et al., 2014), which might affect the task performance.

Further comparison between the fast- and slow-PS networks revealed distinct connectome patterns among the eight functional networks (Fig. 3). The fast-PS network included more within-network connectivity in the motor and visual I networks, while the slow-PS network included more between-network connectivity in the motor-SubC and motor-frontoparietal networks. In other words, a faster PS was associated with more within-network connectivity in the motor and visual I networks. A previous study found that aging was associated with less connectivity within the motor network (Varangis et al., 2019), and older adults exhibiting stronger connectivity within the motor network outperformed their peers in motor and speed functions (Seidler et al., 2015). The visual-related network has also been found to be activated during the SDMT task (Forn et al., 2013). A meta-analysis revealed that the primary visual cortex (BA17, visual I network) plays an essential role in PS and it participates in the detection of visual patterns and visual attention (Silva et al., 2019).

On the other hand, we found more between-network connectivity in the motor-SubC, motor-frontoparietal networks in the slow-PS network, compared to the fast-PS network, which indicated a slower PS. It is suggested that stronger connectivity between the motor and SubC networks was associated with better precision in motor tasks (Schlerf et al., 2014). The cortico-thalamo-cerebellar circuit, including the motor cortex, cerebellum, thalamus and striatum, is involved in subserving the precise motor control function and cognition (Haber and Calzavara, 2009; Manto et al., 2012; Stoodley, 2012). Additionally, cerebellar projections could induce a reduction of excitatory output (inhibition) from the cerebellum through the thalamus to the motor cortex, leading to modified and precise motor control (Daskalakis et al., 2004). Along with these findings, our results indicate that more connectivity between the motor and SubC networks contribute to the precise performance in the SDMT task, however, at the expense of speed. In regard to the motor-frontoparietal connectivity, previous studies found the connectivity between the motor and the frontoparietal networks was negatively related to motor learning (Mary et al., 2016), suggesting that connectivity between the motor and non-motor networks (e.g., the cognitive control network) might affect the motor performance and PS. The increased connectivity between the frontoparietal and motor networks might indicate an enhanced top-down control of motor execution and task operation, due to the lack of sufficient communication within the motor network in older adults (King et al., 2017).

Taken together, the connectome patterns derived from our CPM models in the older adults revealed more within-network connectivity in the fast-PS network, while there was more between-network connectivity in the slow-PS network. Increased within-network connectivity represented higher functional segregation of brain networks; whereas, increased between-network connectivity represented higher functional integration of brain networks (King et al., 2017). Here, functional segregation refers to highly clustered connectivity in networks and functional integration refers to connections between networks that allow integration of information from different networks (Damoiseaux, 2017). Our results might suggest that functional segregation in the key brain networks (i.e., motor networks, SubC networks) plays an important role in supporting certain cognitive functions in older adults. Functional connectivity studies have converged with the observations, demonstrating that older adults have lower network segregation and higher network integration compared to younger adults (Cao et al., 2014; Damoiseaux, 2017; Geerligs et al., 2014). The decreased segregation was found to be associated with age-related decline in motor performance (Cassady et al., 2019; King et al., 2017). Consistent with existing findings, the connectivity patterns generated from our CPM suggest that functional segregation in the motor network is vital for PS functioning in older adults, and higher connections between different networks might indicate an insufficient neural system and a compensatory mechanism to implement certain tasks (Morcom and Johnson, 2015).

4.4. Limitations

Several limitations should be acknowledged in this study. First, our significant findings were generated from rather modest sample sizes (older adults, our sample: $n = 99$; Cam-CAN sample: $n = 91$); however, they can be further verified and validated by studies using a relatively larger sample size. Second, our sample and the Cam-CAN sample significantly differed in their distributions of sex, age and education. Future studies could recruit more homogenous internal and external validation samples. Third, task-fMRI (Greene et al., 2018; Rosenberg et al., 2016) and multimodal brain data (Jiang et al., 2019) have been suggested to improve prediction accuracy. Future work could explore the usefulness of incorporating task-fMRI and multimodal brain data in order to further improve overall model accuracy. Fourth, our study provided preliminary evidence that resting-state connectivity could predict the current PS level in older adults. PS has been found to show an inverted U developmental trajectory throughout the life span (Finkel et al., 2009; Nettelbeck and Burns, 2010). Based on our study, it would be of great interest to predict the change of PS throughout life span by using a longitudinal design in future work.

5. Conclusion

In conclusion, findings of this study clearly indicate that resting-state functional connectivity across multiple neural systems (i.e., the motor, SubC, frontoparietal, medial frontal, default-mode and visual-related networks) can be used to predict PS in older adults. Furthermore, the connectivity patterns generated from the PS-CPM models could be useful for predicting attention and memory performance in older adults. The findings of this study provide evidence that resting-state functional connectivity can be applied to characterizing individual differences in PS in older adults. Further work could help to accumulate evidence on the feasibility and usefulness of applying connectome-based predictive models to understand these neurocognitive abilities. Our results might aid with the clinical diagnosis, prognosis and management of people undergoing aging.

Declaration of Competing Interest

None.

CRediT authorship contribution statement

Mengxia Gao: Conceptualization, Data curation, Formal analysis, Methodology, Writing - original draft, Writing - review & editing. **Clive H.Y. Wong:** Conceptualization, Methodology, Writing - review & editing. **Huiyuan Huang:** Methodology, Writing - review & editing. **Robin Shao:** Writing - review & editing. **Ruiwang Huang:** Writing - review & editing. **Chetwyn C.H. Chan:** Writing - review & editing. **Tatia M.C. Lee:** Conceptualization, Funding acquisition, Project administration, Resources, Supervision, Writing - review & editing.

Acknowledgments

Supplementary materials

Supplementary material associated with this article can be found, in the online version, at doi:10.1016/j.neuroimage.2020.117290.

References

Arnemann, K.L., Chen, A.J.-W., Novakovic-Agopian, T., Gratton, C., Nomura, E.M., D'Esposito, M., 2015. Functional brain network modularity predicts response to cognitive training after brain injury. Neurology 84 (15), 1568–1574.

Betzel, R.F., Byrge, L., He, Y., Goñi, J., Zuo, X.-.N., Sporns, O., 2014. Changes in structural and functional connectivity among resting-state networks across the human lifespan. Neuroimage 102, 345–357.

Bishop, N.A., Lu, T., Yankner, B.A., 2010. Neural mechanisms of ageing and cognitive decline. Nature 464 (7288), 529–535.

Böhr, S., Güllmar, D., Knab, R., Reichenbach, J.R., Witte, O.W., Haueisen, J., 2007. Fractional anisotropy correlates with auditory simple reaction time performance. Brain Res. 1186, 194–202.

Brébion, G., Smith, M.J., Gorman, J.M., Malaspina, D., Sharif, Z., Amador, X., 2000. Memory and schizophrenia: differential link of processing speed and selective attention with two levels of encoding. J. Psychiatr. Res. 34 (2), 121–127.

Buckley, R.F., Schultz, A.P., Hedden, T., Papp, K.V., Hanseeuw, B.J., Marshall, G., et al., 2017. . Functional network integrity presages cognitive decline in preclinical Alzheimer disease. Neurology 89 (1), 29–37.

Bush, G., 2011. Cingulate, frontal, and parietal cortical dysfunction in attention-deficit/hyperactivity disorder. Biol. Psychiatry 69 (12), 1160–1167.

Cao, M., Wang, J.-H., Dai, Z.-J., Cao, X.-Y., Jiang, L.-L., Fan, F.-M., et al., 2014. . Topological organization of the human brain functional connectome across the lifespan. Dev. Cogn. Neuros-Neth 7, 76–93.

Carter, A.R., Astafiev, S.V., Lang, C.E., Connor, L.T., Rengachary, J., Strube, M.J., et al., 2010. Resting interhemispheric functional magnetic resonance imaging connectivity predicts performance after stroke. Ann. Neurol 67 (3), 365–375.

Cassady, K., Gagnon, H., Lalwani, P., Simmonite, M., Foerster, B., Park, D., et al., 2019. . Sensorimotor network segregation declines with age and is linked to GABA and to sensorimotor performance. Neuroimage 186, 234–244.

Chong, J.S.X., Ng, K.K., Tandi, J., Wang, C., Poh, J.-.H., Lo, J.C., et al., 2019. . Longitudinal changes in the cerebral cortex functional organization of healthy elderly. J. Neurosci. 39 (28), 5534–5550.

Damoiseaux, J.S., 2017. Effects of aging on functional and structural brain connectivity. Neuroimage 160, 32–40.

Daskalakis, Z.J., Paradiso, G.O., Christensen, B.K., Fitzgerald, P.B., Gunraj, C., Chen, R., 2004. Exploring the connectivity between the cerebellum and motor cortex in humans. J. Physiol. 557 (2), 689–700.

Deary, I.J., Johnson, W., Starr, J.M., 2010. Are processing speed tasks biomarkers of cognitive aging? Psychol. Aging 25 (1), 219–228.

Deary, I.J., Liewald, D., Nissan, J., 2011. A free, easy-to-use, computer-based simple and four-choice reaction time programme: the Deary-Liewald reaction time task. Behav. Res. Methods 43 (1), 258–268.

Dow, C., Seidenberg, M., Hermann, B., 2004. Relationship between information processing speed in temporal lobe epilepsy and white matter volume. Epilepsy Behav 5 (6), 919–925.

Eckert, M.A., 2011. Slowing down: age-related neurobiological predictors of processing speed. Front. Neurosci. 5, 25.

Eckert, M.A., Keren, N.I., Roberts, D.R., Calhoun, V.D., Harris, K.C., 2010. Age-related changes in processing speed: unique contributions of cerebellar and prefrontal cortex. Front. Hum. Neurosci. 4, 10.

Feng, C., Wang, L., Li, T., Xu, P., 2019. Connectome-based individualized prediction of loneliness. Soc. Cogn. Affect. Neurosci. 14 (4), 353–365.

Ferreira, L.K., Busatto, G.F., 2013. Resting-state functional connectivity in normal brain aging. Neurosci. Biobehav. Rev. 37 (3), 384–400.

Finkel, D., Reynolds, C.A., McArdle, J.J., Hamagami, F., Pedersen, N.L., 2009. Genetic variance in processing speed drives variation in aging of spatial and memory abilities. Dev. Psychol. 45 (3), 820.

Finkel, D., Reynolds, C.A., McArdle, J.J., Pedersen, N.L., 2007. Age changes in processing speed as a leading indicator of cognitive aging. Psychol. Aging 22 (3), 558–568.

Finn, E.S., Shen, X., Scheinost, D., Rosenberg, M.D., Huang, J., Chun, M.M., et al., 2015. . Functional connectome fingerprinting: identifying individuals using patterns of brain connectivity. Nat. Neurosci. 18 (11), 1664–1671.

Folstein, M.F., Folstein, S.E., McHugh, P.R., 1975. "Mini-mental state": a practical method for grading the cognitive state of patients for the clinician. J. Psychiatr. Res. 12 (3), 189–198.

Fong, A.H.C., Yoo, K., Rosenberg, M.D., Zhang, S., Li, C.-S.R., Scheinost, D., et al., 2019. . Dynamic functional connectivity during task performance and rest predicts individual differences in attention across studies. Neuroimage 188, 14–25.

Forn, C., Belloch, V., Bustamante, J.C., Garbin, G., Parcet-Ibars, M.À., Sanjuan, A., et al., 2009. A symbol digit modalities test version suitable for functional MRI studies. Neurosci. Lett 456 (1), 11–14.

Forn, C., Ripollés, P., Cruz-Gómez, A., Belenguer, A., González-Torre, J.A., Avila, C., 2013. Task-load manipulation in the Symbol Digit Modalities Test: an alternative measure of information processing speed. Brain Cogn 82 (2), 152–160.

Fountain-Zaragoza, S., Samimy, S., Rosenberg, M.D., Prakash, R.S., 2019. Connectome-based models predict attentional control in aging adults. Neuroimage 186, 1–13.

Fox, M.D., Greicius, M., 2010. Clinical applications of resting state functional connectivity. Front. Syst. Neurosci. 4, 19.

Gao, S., Greene, A.S., Constable, R.T., Scheinost, D., 2019. Combining multiple connectomes improves predictive modeling of phenotypic measures. Neuroimage 201, 116038.

Gawryluk, J.R., Mazerolle, E.L., Beyea, S.D., D'Arcy, R.C., 2014. Functional MRI activation in white matter during the Symbol Digit Modalities Test. Front. Hum. Neurosci. 8, 589.

Geerligs, L., Renken, R.J., Saliasi, E., Maurits, N.M., Lorist, M.M., 2014. A brain-wide study of age-related changes in functional connectivity. Cereb. Cortex 25 (7), 1987–1999.

Greene, A.S., Gao, S., Scheinost, D., Constable, R.T., 2018. Task-induced brain state manipulation improves prediction of individual traits. Nat Commun 9 (1), 2807.

Haber, S.N., Calzavara, R., 2009. The cortico-basal ganglia integrative network: the role of the thalamus. Brain Res. Bull. 78 (2–3), 69–74.

Hafkemeijer, A., van der Grond, J., Rombouts, S.A., 2012. Imaging the default mode network in aging and dementia. BBA-Mol. Basis Dis. 1822 (3), 431–441.

Hedden, T., Lautenschlager, G., Park, D.C., 2005. Contributions of processing ability and knowledge to verbal memory tasks across the adult life-span. Q. J. Exp. Psychol. [A] 58 (1), 169–190.

Hohenfeld, C., Werner, C.J., Reetz, K., 2018. Resting-state connectivity in neurodegenerative disorders: is there potential for an imaging biomarker? NeuroImage Clin 18, 849–870.

Hsu, W.-.T., Rosenberg, M.D., Scheinost, D., Constable, R.T., Chun, M.M., 2018. Resting-state functional connectivity predicts neuroticism and extraversion in novel individuals. Soc. Cogn. Affect. Neurosci. 13 (2), 224–232.

Iverson, G.L., Lovell, M.R., Collins, M.W., 2005. Validity of ImPACT for measuring processing speed following sports-related concussion. J. Clin. Exp. Neuropsychol. 27 (6), 683–689.

Jangraw, D.C., Gonzalez-Castillo, J., Handwerker, D.A., Ghane, M., Rosenberg, M.D., Panwar, P., et al., 2018. A functional connectivity-based neuromarker of sustained attention generalizes to predict recall in a reading task. Neuroimage 166, 99–109.

Jenkinson, M., Bannister, P., Brady, M., Smith, S., 2002. Improved optimization for the robust and accurate linear registration and motion correction of brain images. Neuroimage 17 (2), 825–841.

Jiang, R., Calhoun, V.D., Cui, Y., Qi, S., Zhuo, C., Li, J., et al., 2019. . Multimodal data revealed different neurobiological correlates of intelligence between males and females. Brain Imaging Behav. 1–15.

Jiang, R., Calhoun, V.D., Zuo, N., Lin, D., Li, J., Fan, L., et al., 2018. . Connectome-based individualized prediction of temperament trait scores. Neuroimage 183, 366–374.

Kennedy, K.M., Raz, N., 2009. Aging white matter and cognition: differential effects of regional variations in diffusion properties on memory, executive functions, and speed. Neuropsychologia 47 (3), 916–927.

King, B., Van Ruitenbeek, P., Leunissen, I., Cuypers, K., Heise, K.-.F., Santos Monteiro, T., et al., 2017. . Age-related declines in motor performance are associated with decreased segregation of large-scale resting state brain networks. Cereb. Cortex 28 (12), 4390–4402.

Koenig, K.A., Lowe, M.J., Harrington, D.L., Lin, J., Durgerian, S., Mourany, L., et al., 2014. . Functional connectivity of primary motor cortex is dependent on genetic burden in prodromal Huntington disease. Brain Connect 4 (7), 535–546.

Lee, H., Baniqued, P.L., Cosman, J., Mullen, S., McAuley, E., Severson, J., et al., 2012. . Examining cognitive function across the lifespan using a mobile application. Comput. Hum. Behav. 28 (5), 1934–1946.

Lee, M.H., Smyser, C.D., Shimony, J.S., 2013. Resting-state fMRI: a review of methods and clinical applications. Am. J. Neuroradiol. 34 (10), 1866–1872.

Lee, T.M., Chan, C.C., 2000. Are trail making and color trails tests of equivalent constructs? J. Clin. Exp. Neuropsychol 22 (4), 529–534.

Lee, T.M., Yuen, K.S., Chan, C.C., 2002. Normative data for neuropsychological measures of fluency, attention, and memory measures for Hong Kong Chinese. J. Clin. Exp. Neuropsychol. 24 (5), 615–632.

Lee, T.M., Zhou, W.-h., Luo, X.-j., Yuen, K.S., Ruan, X.-z., Weng, X.-c., 2005. Neural activity associated with cognitive regulation in heroin users: a fMRI study. Neurosci. Lett. 382 (3), 211–216.

Levitt, T., Fugelsang, J., Crossley, M., 2006. Processing speed, attentional capacity, and age-related memory change. Exp. Aging Res. 32 (3), 263–295.

Lin, Q., Rosenberg, M.D., Yoo, K., Hsu, T.W., O'Connell, T.P., Chun, M.M., 2018. Resting-state functional connectivity predicts cognitive impairment related to alzheimer's disease. Front. Aging Neurosci. 10, 94.

Liu, J., Liao, X., Xia, M., He, Y., 2018. Chronnectome fingerprinting: identifying individuals and predicting higher cognitive functions using dynamic brain connectivity patterns. Hum. Brain Mapp. 39 (2), 902–915.

Lu, P.H., Lee, G.J., Tishler, T.A., Meghpara, M., Thompson, P.M., Bartzokis, G., 2013. Myelin breakdown mediates age-related slowing in cognitive processing speed in healthy elderly men. Brain Cogn 81 (1), 131–138.

Luo, L., Craik, F.I., 2008. Aging and memory: a cognitive approach. Can. J. Psychiatry 53 (6), 346–353.

Manto, M., Bower, J.M., Conforto, A.B., Delgado-García, J.M., Da Guarda, S.N.F., Gerwig, M., et al., 2012. . Consensus paper: roles of the cerebellum in motor control—The diversity of ideas on cerebellar involvement in movement. Cerebellum 11 (2), 457–487.

Mary, A., Wens, V., Op de Beeck, M., Leproult, R., De Tiège, X., Peigneux, P., 2016. Resting-state functional connectivity is an age-dependent predictor of motor learning abilities. Cereb. Cortex 27 (10), 4923–4932.

McLeod, D.R., Griffiths, R.R., Bigelow, G.E., Yingling, J., 1982. An automated version of the digit symbol substitution test (DSST). Behav. Res. Methods Instr. 14 (5), 463–466.

Meskaldji, D.-.E., Preti, M.G., Bolton, T.A., Montandon, M.-.L., Rodriguez, C., Morgen-

thaler, S., et al., 2016. . Prediction of long-term memory scores in MCI based on resting-state fMRI. NeuroImage Clin. 12, 785–795.

Meyer, K., Damasio, A., 2009. Convergence and divergence in a neural architecture for recognition and memory. Trends Neurosci. 32 (7), 376–382.

Morcom, A.M., Johnson, W., 2015. Neural reorganization and compensation in aging. J. Cognit. Neurosci. 27 (7), 1275–1285.

Nettelbeck, T., Burns, N.R., 2010. Processing speed, working memory and reasoning ability from childhood to old age. Pers. Individ. Differ. 48 (4), 379–384.

Panchuelo, R.S., Stephenson, M., Francis, S., Morris, P., 2014. Neural brain activation imaging. Biomedical Imaging. 112–162.

Pievani, M., Filippini, N., Van Den Heuvel, M.P., Cappa, S.F., Frisoni, G.B., 2014. Brain connectivity in neurodegenerative diseases—From phenotype to proteinopathy. Nat. Rev. Neurol. 10 (11), 620–633.

Poldrack, R.A., Huckins, G., Varoquaux, G., 2019. Establishment of best practices for evidence for prediction: a review. JAMA Psychiatry..

Power, J.D., Barnes, K.A., Snyder, A.Z., Schlaggar, B.L., Petersen, S.E., 2012. Spurious but systematic correlations in functional connectivity MRI networks arise from subject motion. Neuroimage 59 (3), 2142–2154.

Prvulovic, D., Bokde, A.L., Faltraco, F., Hampel, H., 2011. Functional magnetic resonance imaging as a dynamic candidate biomarker for Alzheimer's disease. Prog. Neurobiol. 95 (4), 557–569.

Ramos-Nuñez, A.I., Fischer-Baum, S., Martin, R.C., Yue, Q., Ye, F., Deem, M.W., 2017. Static and dynamic measures of human brain connectivity predict complementary aspects of human cognitive performance. Front. Neurosci. 11, 420.

Riccio, C.A., Wolfe, M.E., Romine, C., Davis, B., Sullivan, J.R., 2004. The Tower of London and neuropsychological assessment of ADHD in adults. Archiv. Clin. Neuropsychol. 19 (5), 661–671.

Rosenberg, M.D., Finn, E.S., Scheinost, D., Papademetris, X., Shen, X., Constable, R.T., et al., 2016. . A neuromarker of sustained attention from whole-brain functional connectivity. Nat. Neurosci. 19 (1), 165–171.

Rosenberg, M.D., Scheinost, D., Greene, A.S., Avery, E.W., Kwon, Y.H., Finn, E.S., et al., 2020. . Functional connectivity predicts changes in attention observed across minutes, days, and months. Proc. Natl. Acad. Sci. 117 (7), 3797–3807.

Sakaki, M., Nga, L., Mather, M., 2013. Amygdala functional connectivity with medial prefrontal cortex at rest predicts the positivity effect in older adults' memory. J. Cognit. Neurosci. 25 (8), 1206–1224.

Salthouse, T.A., 1996. The processing-speed theory of adult age differences in cognition. Psychol. Rev. 103 (3), 403–428.

Salthouse, T.A., 2000. Aging and measures of processing speed. Biol. Psychol. 54 (1–3), 35–54.

Salthouse, T.A., 2010. Selective review of cognitive aging. J. Int. Neuropsychol. Soc. 16 (5), 754–760.

Salthouse, T.A., Ferrer-Caja, E., 2003. What needs to be explained to account for age-related effects on multiple cognitive variables? Psychol. Aging 18 (1), 91–110.

Schlerf, J.E., Galea, J.M., Spampinato, D., Celnik, P.A., 2014. Laterality differences in cerebellar–motor cortex connectivity. Cereb. Cortex 25 (7), 1827–1834.

Seidler, R., Erdeniz, B., Koppelmans, V., Hirsiger, S., Mérillat, S., Jäncke, L., 2015. Associations between age, motor function, and resting state sensorimotor network connectivity in healthy older adults. Neuroimage 108, 47–59.

Shafto, M.A., Tyler, L.K., Dixon, M., Taylor, J.R., Rowe, J.B., Cusack, R., et al., 2014. . The Cambridge Centre for Ageing and Neuroscience (Cam-CAN) study protocol: a cross-sectional, lifespan, multidisciplinary examination of healthy cognitive ageing. BMC Neurol. 14 (1), 204.

Shen, X., Finn, E.S., Scheinost, D., Rosenberg, M.D., Chun, M.M., Papademetris, X., et al., 2017. . Using connectome-based predictive modeling to predict individual behavior from brain connectivity. Nat. Protoc. 12 (3), 506–518.

Shen, X., Tokoglu, F., Papademetris, X., Constable, R.T., 2013. Groupwise whole-brain parcellation from resting-state fMRI data for network node identification. Neuroimage 82, 403–415.

Siegel, J.S., Ramsey, L.E., Snyder, A.Z., Metcalf, N.V., Chacko, R.V., Weinberger, K., et al., 2016. . Disruptions of network connectivity predict impairment in multiple behavioral domains after stroke. Proc. Natl. Acad. Sci. 113 (30), E4367–E4376.

Silva, P., Spedo, C., Baldassarini, C., Benini, C., Ferreira, D., Barreira, A., et al., 2019. . Brain functional and effective connectivity underlying the information processing speed assessed by the Symbol Digit Modalities Test. Neuroimage 184, 761–770.

Silva, P., Spedo, C., Barreira, A., Leoni, R., 2018. Symbol digit modalities test adaptation for magnetic resonance imaging environment: a systematic review and meta-analysis. Mult. Scler. Relat. Dis. 20, 136–143.

Smith, A., 1982. Symbol Digit Modalities Test. Western Psychological Services, Los Angeles, CA.

Smith, S.M., Vidaurre, D., Beckmann, C.F., Glasser, M.F., Jenkinson, M., Miller, K.L., et al., 2013. . Functional connectomics from resting-state fMRI. Trends Cogn. Sci. 17 (12), 666–682.

Steiger, J.H., 1980. Tests for comparing elements of a correlation matrix. Psychol. Bull. 87 (2), 245.

Stoodley, C.J., 2012. The cerebellum and cognition: evidence from functional imaging studies. Cerebellum 11 (2), 352–365.

Taylor, J.R., Williams, N., Cusack, R., Auer, T., Shafto, M.A., Dixon, M., et al., 2017. . The Cambridge Centre for Ageing and Neuroscience (Cam-CAN) data repository: structural and functional MRI, MEG, and cognitive data from a cross-sectional adult lifespan sample. Neuroimage 144, 262–269.

Trahan, D.E., Larrabee, G.J., 1988. Continuous visual memory test: professional manual. Psychol. Ass. Res. 19 pages.

Van Den Heuvel, M.P., Pol, H.E.H., 2010. Exploring the brain network: a review on resting-state fMRI functional connectivity. Eur. Neuropsychopharmacol. 20 (8), 519–534.

Van Dijk, K.R., Hedden, T., Venkataraman, A., Evans, K.C., Lazar, S.W., Buckner, R.L.,

2010. Intrinsic functional connectivity as a tool for human connectomics: theory, properties, and optimization. J. Neurophysiol. 103 (1), 297–321.

Varangis, E., Habeck, C., Razlighi, Q., Stern, Y., 2019. The effect of aging on resting state connectivity of predefined networks in the brain. Front. Aging Neurosci. 11, 234.

Villemagne, V.L., Burnham, S., Bourgeat, P., Brown, B., Ellis, K.A., Salvado, O., et al., 2013. . Amyloid β deposition, neurodegeneration, and cognitive decline in sporadic Alzheimer's disease: a prospective cohort study. Lancet Neurol. 12 (4), 357–367.

Wu, E.X., Liaw, G.J., Goh, R.Z., Chia, T.T., Chee, A.M., Obana, T., et al., 2020. . Overlapping attentional networks yield divergent behavioral predictions across tasks: neuromarkers for diffuse and focused attention? Neuroimage 209, 116535.

Wu, T., Zang, Y., Wang, L., Long, X., Hallett, M., Chen, Y., et al., 2007. . Aging influence on functional connectivity of the motor network in the resting state. Neurosci. Lett. 422 (3), 164–168.

Yan, C.-.G., Cheung, B., Kelly, C., Colcombe, S., Craddock, R.C., Di Martino, A., et al., 2013. . A comprehensive assessment of regional variation in the impact of head micromovements on functional connectomics. Neuroimage 76, 183–201.

Yan, C.-G., Wang, X.-.D., Zuo, X.-.N., Zang, Y.-.F., 2016. DPABI: data processing & analysis for (resting-state) brain imaging. Neuroinformatics 14 (3), 339–351.

Yeung, P., Wong, L., Chan, C., Leung, J., Yung, C., 2014. A validation study of the hong kong version of montreal cognitive assessment (HK-MoCA) in Chinese older adults in Hong Kong. Hong Kong Med. J. 20 (6), 504–510.

Yu, J., Lam, C.L., Man, I.S., Shao, R., Lee, T.M., 2020. Multi-session anodal prefrontal transcranial direct current stimulation does not improve executive functions among older adults. J. Int. Neuropsychol. Soc. 26 (4), 372–381.

Zaremba, D., Kalthoff, I.S., Förster, K., Redlich, R., Grotegerd, D., Leehr, E.J., et al., 2019. . The effects of processing speed on memory impairment in patients with major depressive disorder. Prog. Neuro-Psychopharmacol. Biol. Psychiatry 92, 494–500.

Zonneveld, H.I., Pruim, R.H., Bos, D., Vrooman, H.A., Muetzel, R.L., Hofman, A., et al., 2019. . Patterns of functional connectivity in an aging population: the Rotterdam study. Neuroimage 189, 432–444.